tvst

Article

Optical Coherence Tomography Angiography Projection Artifact Removal: Impact on Capillary Density and Interaction with Diabetic Retinopathy Severity

Mohamed Ashraf[1], Konstantina Sampani[1,2], Omar Abu-Qamar[1], Jerry Cavallerano[1,3], Paolo S. Silva[1,3], Lloyd Paul Aiello[1,3], and Jennifer K. Sun[1,3]

[1] Beetham Eye Institute, Joslin Diabetes Center, Boston, Massachusetts, USA
[2] Department of Medicine, Harvard Medical School, Boston, Massachusetts, USA
[3] Department of Ophthalmology, Harvard Medical School, Boston, Massachusetts, USA

Correspondence: Jennifer K. Sun, Beetham Eye Institute, Joslin Diabetes Center, One Joslin Place, Boston, MA 02215, USA. e-mail: jennifer.sun@joslin.harvard.edu

Received: February 6, 2020
Accepted: March 29, 2020
Published: June 5, 2020

Keywords: optical coherence tomography angiography; retina; diabetic retinopathy imaging

Citation: Ashraf M, Sampani K, Abu-Qamar O, Cavallerano J, Silva PS, Aiello LP, Sun JK. Optical coherence tomography angiography projection artifact removal: Impact on capillary density and interaction with diabetic retinopathy severity. Trans Vis Sci Tech. 2020;9(7):10, https://doi.org/10.1167/tvst.9.7.10

Purpose: The purpose of this study was to assess how projection artifact removal (PAR) alters optical coherence tomography angiography (OCTA) assessment of superficial capillary plexus (SCP) and deep capillary plexus (DCP) in eyes of patients with diabetes.

Methods: We acquired 3 × 3 mm scans with RTVue-XR Avanti (Optovue, Inc., Fremont, CA), which were analyzed with PAR software (PAROCTA) and without (non-PAROCTA). SCP, DCP, and full thickness retina vascular density (VD) and vessel linear density (VLD) were manually calculated using ImageJ (version 1.51). Adjusted flow index (AFI) was manually assessed for full thickness images.

Results: Among 323 eyes of 194 patients (no diabetic retinopathy [DR]: 28 eyes; mild nonproliferative DR (NPDR): 96 eyes; moderate: 82 eyes; severe: 32 eyes; and proliferative DR [PDR]: 81 eyes), SCP VD and VLD were lower with PAROCTA than with non-PAROCTA only in eyes with moderate (VD: $P = 0.017$; VLD: $P = 0.046$), severe ($P = 0.016$; $P = 0.009$), and PDR ($P < 0.001$; $P = 0.002$). DCP VD and VLD were higher with PAROCTA as compared to non-PAROCTA only in eyes with no DR (VD and VLD: $P < 0.001$), mild (VD and VLD: $P < 0.001$), moderate (VD: $P = 0.005$; and VLD: $P < 0.001$), and severe (VD: $P = 0.009$; VLD: $P < 0.001$). Full thickness PAROCTA and non-PAROCTA VD and VLD differed only in eyes with no DR where PAROCTA estimates were higher (VD: $P = 0.009$; VLD: $P = 0.02$). PAROCTA AFI was lower than non-PAROCTA AFI for all DR severity levels ($P < 0.001$) except no DR.

Conclusions: Although differential effects of PAROCTA software are expected on SCP versus DCP measurements, these findings also suggest an interaction between PAROCTA and DR severity on assessment of VD. Conclusions from previous studies that have not corrected VD with PAR software should be carefully reviewed with regard to the role of specific vascular layers in DR.

Translational Relevance: Previous OCTA studies that have not corrected VD with PAR software should be carefully reviewed with regard to the role of individual vascular layers in differing severity levels of DR.

Introduction

Optical coherence tomography angiography (OCTA) is a rapidly developing noninvasive imaging modality that allows quick and detailed evaluation of retinal vascular perfusion.[1] This technology holds great promise for the identification of early retinal vascular disease, including diabetic retinopathy (DR) with the potential for determining risk for future DR progression.[2,3] Although a major advantage of this technology is that the various retinal vascular

plexuses can be identified, a variety of artifacts are now known to exist when using early software versions to determine vascular density.[4,5] Current software modifications attempt to account for and remove these artifacts; however, these programs have not been rigorously evaluated across the full range of DR severity.[6,7] In order to interpret OCTA vascular density results accurately, it will be critical to understand whether this artifact removal yields consistent results across all DR severity levels or if future OCTA studies should include eyes across the spectrum of DR rather than generalizing from a specific DR subgroup.

Among the most important OCTA image artifacts are projection artifacts, oftentimes referred to as decorrelation tails. These occur due to superficial layer blood flow and vascular structures casting shadows onto deeper layers, generating false vascular networks when visualizing en face images. These artifacts may be erroneously interpreted as flow by current OCTA algorithms and have been shown to quantitatively alter measurements, especially of the deep vascular layers.[5]

Several strategies have been implemented to reduce the effects of projection artifacts, which range from slab removal to projection resolved OCTA (PR-OCTA).[8,9] Recently, Garrity et al. described the use of a novel 3-D projection artifact removal software (PAROCTA) currently available as part of the AngioVue software (RTvue XR Avanti; Optovue, Fremont, CA).[10] This algorithm works similarly to PR-OCTA, previously described by Zhang et al., in that suppression of projection artifacts is achieved based on normalized OCTA intensity, defined as voxel-based intensity divided by optical coherence tomography (OCT) intensity.[8] When the normalized OCTA intensity of a voxel is greater than the normalized OCTA intensity anterior to it along the axial plane, the voxel is considered to be a non-projection artifact signal and its original OCTA intensity is maintained; otherwise, the voxel is considered to be a projection artifact signal and its OCTA intensity is suppressed to zero. With Optovue 3D-PAR, projection artifact removal works in a similar fashion but, in addition to the OCT and OCTA intensity, it uses additional information, such as the intensity gradient along the Z-axis, and projection artifacts are suppressed to the level of background noise and not to zero.

Many earlier studies looking at changes in vascular density measurements in DR did not use projection artifact removal software.[11–19] Since the introduction of 3-D PAROCTA, it has been increasingly used in clinical studies.[20–23] However, these studies have not compared measurements obtained using projection artifact removal software to those obtained without projection artifact removal. Thus, although it is assumed that the introduction of projection artifact removal may alter deeper layer measurements, whether these differences are significant or clinically relevant has yet to be determined. It is also unknown whether the algorithm leads to different effects in eyes with increasing DR severity. Indeed, increasing DR severity has been associated with worsening abnormalities in both the superficial and deep vascular plexus density.[12,13,15] Understanding these differential effects will enable more precise interpretation of previous non-PAROCTA DR studies, some of which focused on early DR,[2,24] whereas others included more advanced DR severity.[12,15]

Thus, the purpose of this study is to compare quantitative vessel density measurements in the same eyes using PAROCTA and non-PAROCTA software. We evaluated eyes with no DR to proliferative diabetic retinopathy (PDR) to assess how PAROCTA alters the assessment of the superficial capillary plexus (SCP) and deep capillary plexus (DCP).

Methods

This retrospective chart review study was approved by the Joslin Diabetes Center Institutional Review Board and adhered to the tenets of the Declaration of Helsinki. Eligible patients were adults with type 1 or 2 diabetes mellitus (DM) who had received OCTA, spectral domain optical coherence tomography (SDOCT), and 200-degree ultrawide field imaging (California/TX200; Optos PLC, Dunfermline, UK) for clinical or research purposes between February 15, 2016, and November 15, 2017. Study eyes spanned the full range of DR severity. Exclusion criteria included spherical equivalent (SE) of <-6 diopters or $>+3$ diopters (D), non-diabetic macular pathology (e.g. retinal vein or artery occlusion, age-related macular degeneration, etc.), glaucoma, or history of pars plana vitrectomy or a history of antivascular endothelial growth factor treatment (anti-VEGF). Also excluded were eyes with macular edema (defined as central subfield thickness [CST] $>$ 320 micrometers [μm] in men and 305 μm in women), vitreomacular traction, epiretinal membranes, or cystoid spaces in the central 3×3 mm scans.

Standardized data collection forms were used to record patient and eye characteristics, including SE, lens status, HbA1c levels measured within 3 months of the date of imaging, duration of DM, and type of DM. Given that absence of macular edema was an inclusion criterion, SDOCT (Heidelberg Engineering

Co., Heidelberg, Germany) was evaluated for significant segmentation errors, and any errors were manually adjusted to ensure that the CST was accurate. Poor quality scans where adequate segmentation could not be obtained were excluded because the CST could not be accurately calculated. Although Optovue measurements could have been utilized for CST measurements, given that previous multicenter, interventional trials for diabetic macular edema (DME) have utilized either Heidelberg or Zeiss OCT devices and their respective cut-offs, this study opted to use the Heidelberg OCT device for that purpose.[25] Nonsimultaneous stereoscopic, on axis, non-steered, 200-degree ultrawide field (UWF) color fundus images (Optos PLC) were assessed by a grader clinical trial certified for evaluating UWF images (M.A.) as either no DR (NDR), mild nonproliferative diabetic retinopathy (NPDR), moderate NPDR, severe NPDR, or PDR based on the clinical early treatment diabetic retinopathy study (ETDRS) severity scale in a manner previously documented to compare favorably with gold standard seven field ETDRS photographs.[26,27]

OCTA Image Acquisition

OCTA imaging was performed using the RTVue XR Avanti spectral-domain OCT device (Optovue). This device uses a light source of 840 nm, with an A-scan rate of 70,000 scans per second. The macular region was scanned using 3 × 3 mm scans, each consisting of 304 × 304 line scans. The AngioVue software uses the split spectrum amplitude-decorrelation angiography (SSADA) algorithm, which has previously been described.[1]

OCTA images of the SCP, DCP, and full thickness retina were extracted using both non-PAROCTA (version 2016.2.0.35) and PAROCTA (version 2017.1.0.149) software versions. In the PAROCTA version, images were automatically segmented using the built-in software to define the SCP and DCP. For the SCP, the inner boundary of the en face image segment was set at the internal limiting membrane (ILM), and the outer boundary was set 10 µm above the inner plexiform layer (IPL). For the DCP, the inner boundary was set 10 µm above the IPL and the outer boundary was set 10 µm beneath the outer plexiform layer (OPL). In the non-PAROCTA version, the built-in algorithm segments the SCP slab from 3 µm posterior to the ILM to 15 µm posterior to the IPL. The DCP slab was segmented from 15 µm posterior to the IPL to 70 µm posterior to the IPL. For each study eye, individual scans from both versions of the software were manually assessed to ensure no significant segmentation errors or artifacts. No manual corrections were made for the Optovue OCTA images; however, eyes with significant segmentation errors were excluded. Poor quality images with a signal strength index (SSI) < 60, a quality index (QI) < 6, or significant motion artifact were also excluded from analysis. A total of 31 of 354 eyes were excluded from the final analysis due to significant motion artifact or OCTA segmentation errors.

OCTA Image Processing

The en face OCTA images were exported to ImageJ, an external imaging software (National Institutes of Health, Bethesda, MD). Images were binarized using a previously validated technique.[12,28,29] In brief, after using a "top hat filter," images were duplicated, with one image being processed using a hessian filter followed by global Huang thresholding and the second image being binarized using local median thresholding. Only pixels common to both images were used to generate a final image that was analyzed quantitatively.

For each OCTA image, vessel density (VD) was calculated as the percentage of area occupied by vessels. The binarized images were then skeletonized, which generates a 1-pixel wide vascular tree and provides an indication of the total length of the vessels independent of their diameter. Vascular length density (VLD) was then calculated as a percentage of the total vascular length divided by the total area. Adjusted flow index (AFI) was evaluated for full thickness images only, using a previously validated technique.[30] The average pixel intensity of the fovea was determined and average pixel intensity for all vessels above this threshold was calculated to determine the AFI for the full image.

Identifying Origin of Differences Between PAROCTA and non-PAROCTA in Deeper Vascular Layers

In order to identify pixels unique to PAROCTA, binarized images obtained using non-PAROCTA were subtracted from PAROCTA images. To identify pixels unique to non-PAROCTA, PAROCTA binarized images were subtracted from non-PAROCTA images. To identify whether these differences originated from the SCP or the DCP, images were converted to green pixels and overlaid on SCP images (red) of the same eye. Similar pixels were identified as yellow (Fig. 1).

Statistics

The Shapiro–Wilk test was used to test for normality of distribution. Analysis of variance with post hoc

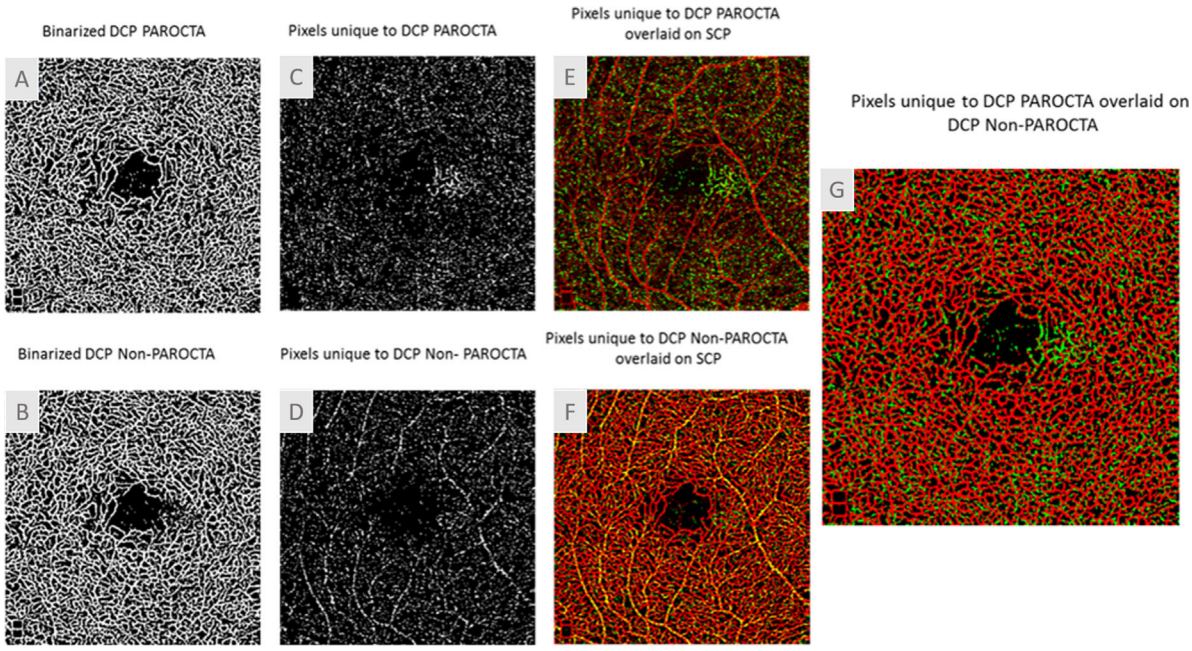

Figure 1. Identifying differences in the deep capillary plexus (DCP) between projection artifact removal (PAROCTA) and non-PAROCTA processed eyes. (**A, B**) Binarized images of the DCP using PAROCTA and non-PAROCTA versions of the software. (**C**) Pixels exclusive to PAROCTA obtained by subtracting the non-PAROCTA image from the PAROCTA image. (**D**) Pixels exclusive to non-PAROCTA obtained by subtracting the PAROCTA image from the non-PAROCTA image. (**E, F**) Pixels unique to each version of the software (green) overlaid on the superficial capillary plexus (SCP) (Red) with common pixels shown in yellow, demonstrating that differences unique to non-PAROCTA are mainly projection artifacts from the SCP while those exclusive from PAROCTA originate from the DCP. (**G**) Pixels unique to PAROCTA (green) when overlaid on the non-PAROCTA DCP (red) demonstrate "recovery" of finer capillaries not previously visualized on non-PAROCTA.

Bonferroni correction was used to compare SE, SSI, QI, and CST between different DR severity levels. Comparison of VD and VLD measurements for different DR severity levels between PAROCTA and non-PAROCTA images was done using the Kruskal–Wallis test for the SCP and analysis of variance for the DCP with post hoc Bonferroni correction. When comparing non-PAROCTA and PAROCTA measurements, paired *t*-test or Wilcoxon Rank was used depending on the normality of distribution. Chi-square test was performed to compare the categorical groups. Pearson correlations were performed when looking at the correlation between VD measurements of the SCP and DCP as well as between manual and automatic SCP measurements. SPSS statistical software version 23 (SPSS, Inc., IBM Company, Chicago, IL) was used for statistical analysis. A P value of < 0.05 was considered statistically significant.

Results

The study included 323 eyes of 194 patients. Mean ± SD age was 51.5 ± 14.3 years, hemoglobin HbA1c was 8.2 ± 1.1%, and diabetes duration was 7.5 ± 1.3 years. In this cohort, 42% were women and 71% had type 1 diabetes. There were no significant differences in age, HbA1c, or duration of DM between patients with different DR severity levels (Table 1). There were also no significant differences in SE, CST, SSI, or QI between the different DR severity levels. As expected, both VD and VLD measurements decreased with increasing DR severity ($P < 0.001$ for trend test of all VD and VLD assessments: SCP and DCP, as well as PAROCTA and non-PAROCTA).

When assessing the effect of projection artifact removal on vascular measurements across DR severity, SCP VD and VLD were significantly lower with PAROCTA than with non-PAROCTA for eyes with moderate NPDR (VD: $P = 0.017$; VLD: $P = 0.046$), severe NPDR (VD: $P = 0.016$; VLD: $P = 0.009$) and PDR (VD: $P < 0.001$; VLD: $P = 0.002$), but not for eyes with no DR or mild NPDR (Table 2, Fig. 2, Fig. 3). DCP VD and VLD were significantly higher with PAROCTA compared to non-PAROCTA in eyes with no DR (VD and VLD: $P < 0.001$), mild NPDR (VD and VLD: $P < 0.001$), moderate NPDR (VD: $P = 0.005$; VLD: $P < 0.001$) and severe NPDR (VD: $P = 0.009$; VLD: $P < 0.001$), but not in eyes with

Table 1. Patient and Ocular Characteristics by DR Severity

DR Severity	No DR	Mild NPDR	Moderate NPDR	Severe NPDR	PDR
Patient characteristics					
Patients, *N*	14	66	48	19	44
Age, ymean ± SD	55.79 ± 14.84	55.06 ± 15.04	55.10 ± 13.09	46.58 ± 11.55	47.48 ± 14.25
HbA1c, %mean ± SD	7.15 ± 0.84	8.13 ± 1.75	8.1 ± 1.9	8.38 ± 1.17	8.68 ± 1.26
Duration of DM, ymean ± SD	18.23 ± 20.14	29.51 ± 17.54	34.77 ± 13.78	25.58 ± 13.25	30.66 ± 15.53
Type DM, *N* (%)					
type 1	10 (71.4)	42 (63.6)	37 (78.7)	14 (73.7)	35 (79.5)
type 2	4 (28.6)	24 (36.4)	10 (21.3)	5 (26.3)	9 (27.4)
Ocular characteristics					
Eyes *N* (%)	28 (8.7)	96 (29.7)	82 (25.4)	32 (9.9)	81 (25.1)
SE, mean ± SD	−2.47 ± 3.27	−1.00 ± 2.10	−1.01 ± 2.11	−0.95 ± 1.55	−1.64 ± 2.44
SSI, mean ± SD	72.08 ± 8.03	72.27 ± 7.93	71.03 ± 8.36	68.99 ± 7.62	69.71 ± 7.51
QI, mean ± SD	7.54 ± 1.26	7.71 ± 1.06	7.46 ± 1.24	7.5 ± 1.13	7.38 ± 1.94
CST, µmmean ± SD	264.82 ± 57.24	257.89 ± 67.36	259.86 ± 80.95	272.16 ± 74.03	275.07 ± 48.6
Pseudophakia, *N* (%)	5 (17.86)	13 (13.54)	16 (24.24)	1 (2.7%)	10 (14.08)

Continuous variables compared with ANOVA with pairwise comparisons and Bonferroni correction. Categorical Values compared using Chi-square test. Significance set at $P < 0.05$.

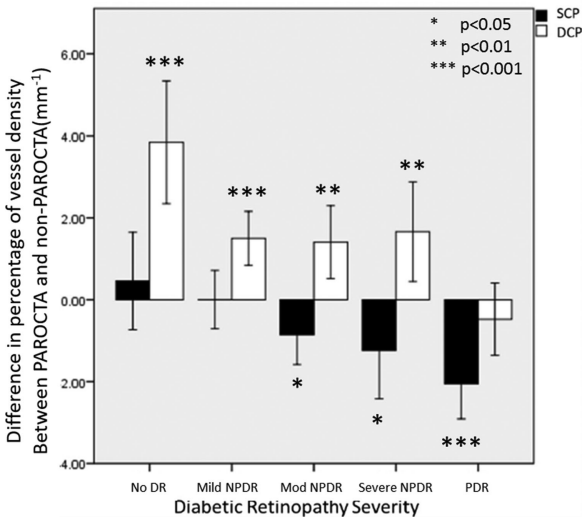

Figure 2. Differences between PAROCTA and non-PAROCTA vessel density measurements in superficial (SCP) and deep capillary plexus (DCP) across different DR severity levels.

PDR. Images processed using non-PAROCTA had significantly more projection artifacts visualized in the deeper layers in early DR (no DR, mild and moderate NPDR; Fig. 4) compared to more advanced DR (severe NPDR and PDR; Fig. 4). Qualitatively, the SCP VD appeared similar on en face images obtained using either PAROCTA or non-PAROCTA in early DR (Fig. 4) but appeared denser on non-PAROCTA images compared to PAROCTA in eyes with PDR (Fig. 4).

For full thickness VD measurements, there was a significant difference in eyes with no DR ($P = 0.003$) and moderate NPDR ($P = 0.032$), but no difference in eyes with mild NPDR, severe NDPR, and PDR. When evaluating VLD, there was a significant different between PAROCTA and non-PAROCTA measurements only in eyes with no DR ($P = 0.010$; Table 3). The AFI using PAROCTA was significantly lower compared to non-PAROCTA in all DR severity levels except no DR.

Using non-PAROCTA, there was strong correlation between SCP and DCP VD across all DR severity levels (Fig. 5). The highest correlation of VD in the SCP and DCP was seen in in eyes with mild ($r = 0.62$, $P < 0.001$) and moderate ($r = 0.68$, $P < 0.001$) NPDR and the lowest correlation was observed in eyes with no DR ($r = 0.48$, $P = 0.010$) and severe NPDR ($r = 0.56$, $P < 0.001$). However, when using PAROCTA, only eyes with severe NPDR showed a VD correlation ($r = 0.32$, $P = 0.036$), whereas other DR severity levels showed no statistically significant correlation. When assessing the correlation between automatic and manual SCP VD measurements, both PAROCTA ($r = 0.71$, $P < 0.001$) and non-PAROCTA ($r = 0.69$, $P < 0.001$) measurements were highly correlated (Fig. 5).

Pixels unique to PAROCTA DCP originated from the deeper layers while those unique to non-PAROCTA were projection artifacts (Fig. 1). When overlaid

Table 2. Comparison Between Manual non-PAROCTA and PAROCTA VD Measurements Across DR Severity

	SCP VD (%) (Mean ± SD)			SCP VLD (%) (Mean ± SD)			DCP VD (%) (Mean ± SD)			DCP VLD (%) (Mean ± SD)		
DR severity	non-PAR	PAROCTA	*P* value	non-PAR	PAROCTA	*P* value	non-PAR	PAROCTA	*P* value	non-PAR	PAROCTA	*P* value
No DR	35.36 ± 2.97	36.2 ± 2.783	0.387	17.81 ± 1.05	18.21 ± 1.53	0.524	35.88 ± 2.82	40.24 ± 4.31	<0.001*	18.78 ± 0.94	21.47 ± 2.95	<0.001*
Mild NPDR	34.91 ± 2.34	34.91 ± 4.39	0.99	17.38 ± 1.38	17.56 ± 2.75	0.37	35.85 ± 3.86	37.69 ± 3.97	<0.001*	18.51 ± 1.21	19.57 ± 2.65	<0.001*
Moderate NPDR	34.24 ± 2.45	33.38 ± 3.87	0.017*	16.87 ± 0.11	16.5 ± 2.4	0.046*	35.32 ± 4.12	37.12 ± 4.58	0.005*	18.15 ± 1.19	19.55 ± 2.96	<0.001*
Severe NPDR	33.8 ± 2.12	32.56 ± 3.75	0.016*	16.5 ± 1.19	15.72 ± 2.19	0.009*	35.17 ± 2.56	36.83 ± 3.62	0.009*	17.91 ± 1.25	19 ± 2.23	<0.001*
PDR	32.77 ± 3.32	30.75 ± 5.02	<0.001*	15.85 ± 1.57	15.1 ± 2.76	0.002*	33.96 ± 2.29	33.47 ± 4.93	0.273	17.04 ± 1.24	16.96 ± 2.94	0.783

Non-PAR and PAR SCP parameters were compared using Wilcoxon–Rank and DCP parameters compared with paired *t*-test. Significance < 0.05.

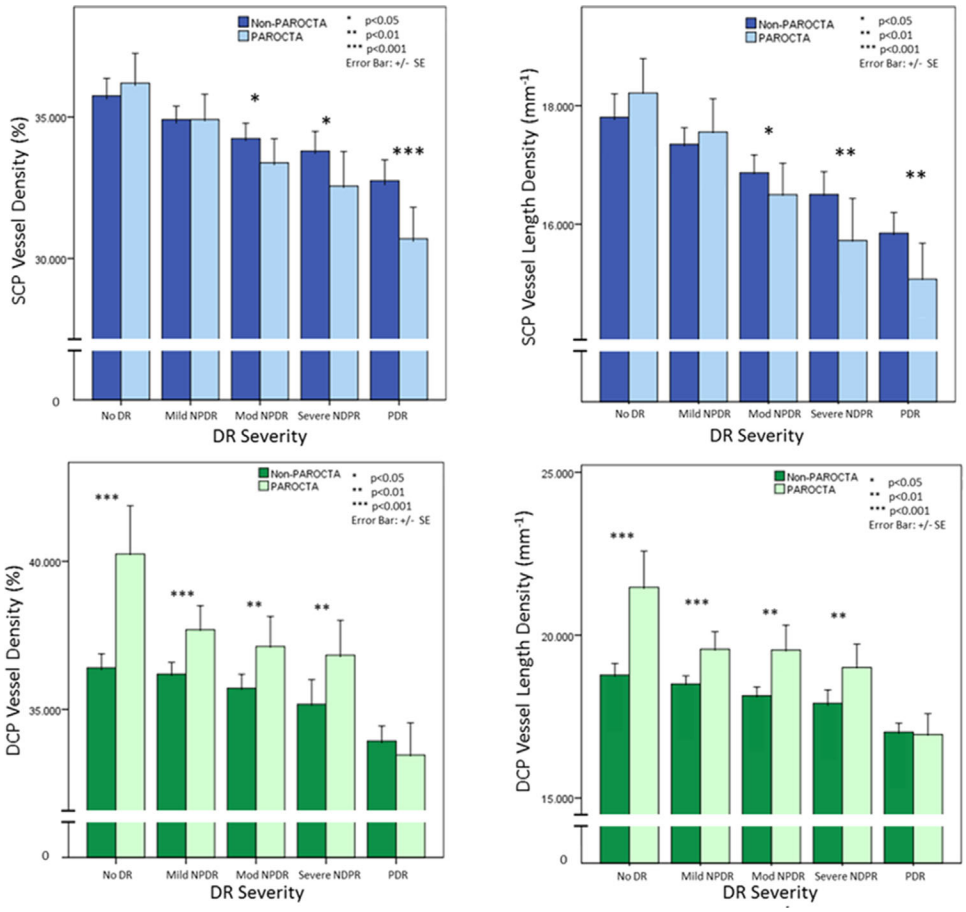

Figure 3. Bar graphs demonstrating the differences between PAROCTA and non-PAROCTA in different diabetic retinopathy (DR) severity levels. The upper row illustrates changes in the SCP demonstrating that with increasing DR severity levels vessel density (VD) and vessel length density (VLD) decreases in both versions of the software. PAROCTA measurements are lower for both the VD and VLD, with increasing disparity with higher DR severity levels. The lower row illustrates changes in the DCP demonstrating similar trends to the SCP. However, PAROCTA measurements are greater for both the VD and VLD, with greater disparity in milder DR.

Table 3. Comparison Between PAROCTA and non-PAROCTA Vessel Density, Vessel Linear Density and Adjusted Flow Index in Full Thickness OCTA Slabs

	Vessel Density (%) (Mean ± SD)			Vessel Length Density (%) (Mean ± SD)			AFI (Mean ± SD)		
DR Severity	non-PAR	PAROCTA	*P* Value	non-PAR	PAROCTA	*P* Value	non-PAR	PAROCTA	*P* Value
No DR	40.91 ± 3.77	42.78 ± 2.25	0.003*	21.56 ± 2.15	22.24 ± 2.01	0.010*	0.55 ± 0.02	0.54 ± 0.02	0.183
Mild NPDR	40.94 ± 3.23	40.80 ± 3.17	0.607	21.26 ± 1.93	21.08 ± 1.88	0.111	0.56 ± 0.02	0.55 ± 0.02	0.001*
Moderate NPDR	39.80 ± 3.61	40.44 ± 3.20	0.032*	20.51 ± 2.01	20.69 ± 1.88	0.190	0.56 ± 5.75	0.54 ± 0.02	<0.001*
Severe NPDR	40.16 ± 3.04	39.83 ± 3.39	0.413	20.48 ± 1.88	20.23 ± 1.97	0.141	0.57 ± 0.019	0.55 ± 0.03	<0.001*
PDR	37.45 ± 4.13	37.58 ± 3.82	0.694	18.96 ± 2.28	18.91 ± 2.11	0.728	0.56 ± 0.02	0.55 ± 0.02	0.007*

Non-PAR and PAROCTA measurements were compared using paired *t*-test. *Significance set at $P < 0.05$.

on DCP non-PAROCTA images, PAROCTA DCP demonstrated fine DCP networks not previously visualized on non-PAROCTA. Furthermore, significantly more deeper capillaries are visualized using PAROCTA in eyes with no DR compared to eyes with PDR (Fig. 6).

Discussion

Differential effects of PAROCTA software analysis are expected between SCP and DCP measurements because the role of the software is to reduce artifacts

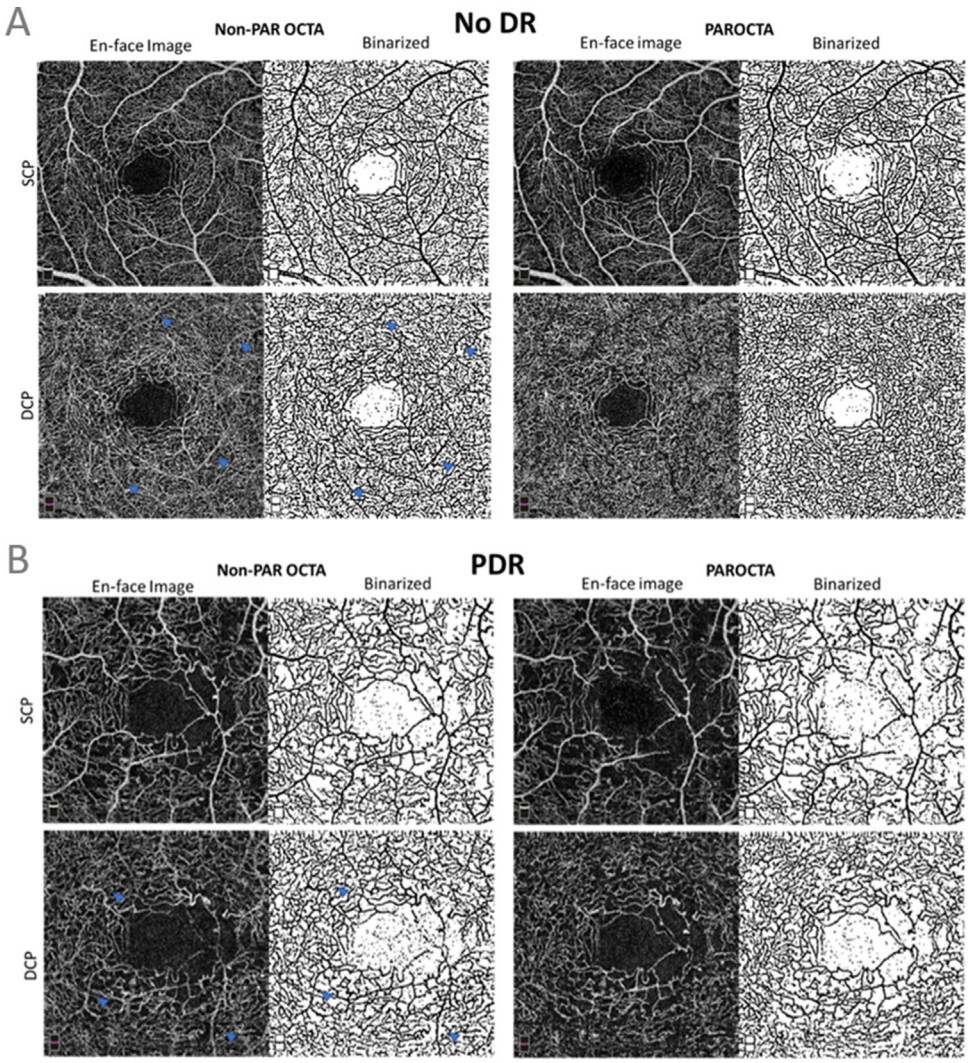

Figure 4. (**A**) Figure illustrating differences in the superficial capillary plexus (SCP) and deep capillary plexus (DCP) between projection artifact removal optical coherence tomography angiography (PAROCTA) and non-PAROCTA in an eye with no DR. The SCP appears to have similar vessel density in both PAR and non-PAROCTA images. The DCP using non-PAROCTA has many projection artifacts (*blue arrowheads*) and appears less dense compared to the PAROCTA image. (**B**) Image showing the difference between projection artifact removal optical coherence tomography angiography (PAROCTA) and non-PAROCTA in an eye with proliferative diabetic retinopathy (PDR) showing decreased vessel density (VD) in the superficial capillary plexus (SCP) with similar VD in the deep capillary plexus (DCP). Due to a decrease in SCP VD, fewer projection artifacts (*blue arrowheads*) are visible in the DCP in this eye with PDR compared to the eye with no DR.

in the DCP induced by the SCP. Our findings characterize those differences and also identify an interaction between PAROCTA and DR severity on assessment of vascular density. SCP VD and VLD measurements in eyes with moderate NPDR or worse were significantly lower after projection artifact removal, with the most significant differences occurring in eyes with PDR. However, SCP VD assessment was not significantly altered in eyes with no DR or mild NPDR. In contrast, DCP VD and VLD measurements were significantly greater when using PAROCTA across all DR severity levels except PDR, with the greatest differences observed in eyes with less severe DR.

Across the all DR severity levels (no DR to PDR), SCP, and DCP VD measurements demonstrate little to no correlation with each other after incorporation of projection artifact removal, whereas non-PAROCTA images demonstrated significant correlations between SCP and DCP VD measurements. Furthermore, effects of PAR were different at different DR severity levels. These findings imply that PAROCTA is effective at removing superficial vascular plexus artifacts in the assessment of the deeper vascular layers. These results also suggest that there may be a disassociation between SCP and DCP vascular metrics within the same eye. Changes in the SCP and DCP with

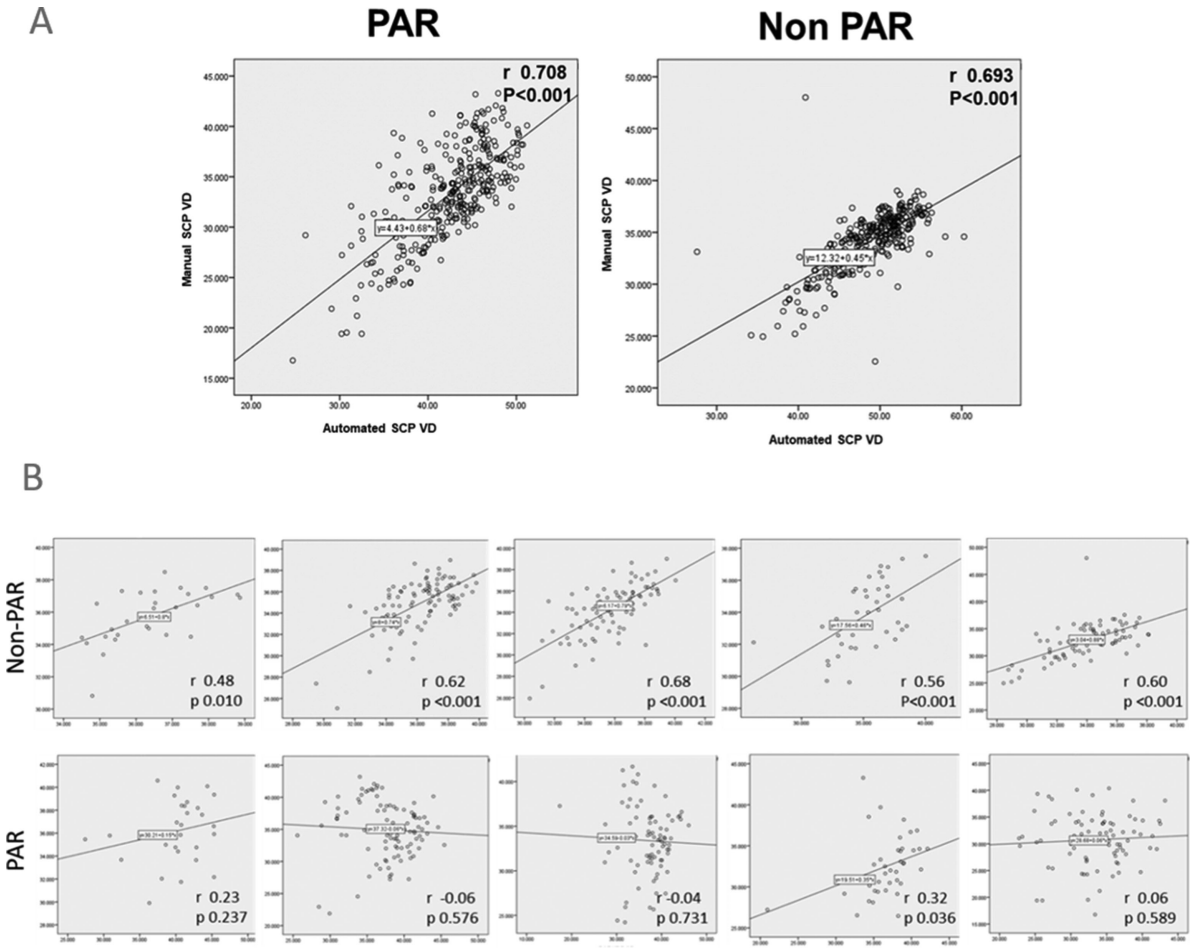

Figure 5. (**A**) Correlation between superficial (SCP) and deep capillary plexus (DCP) vessel density across all DR severity levels. (**B**) Correlation between automatic and manual superficial capillary plexus vessel density in eyes with DR.

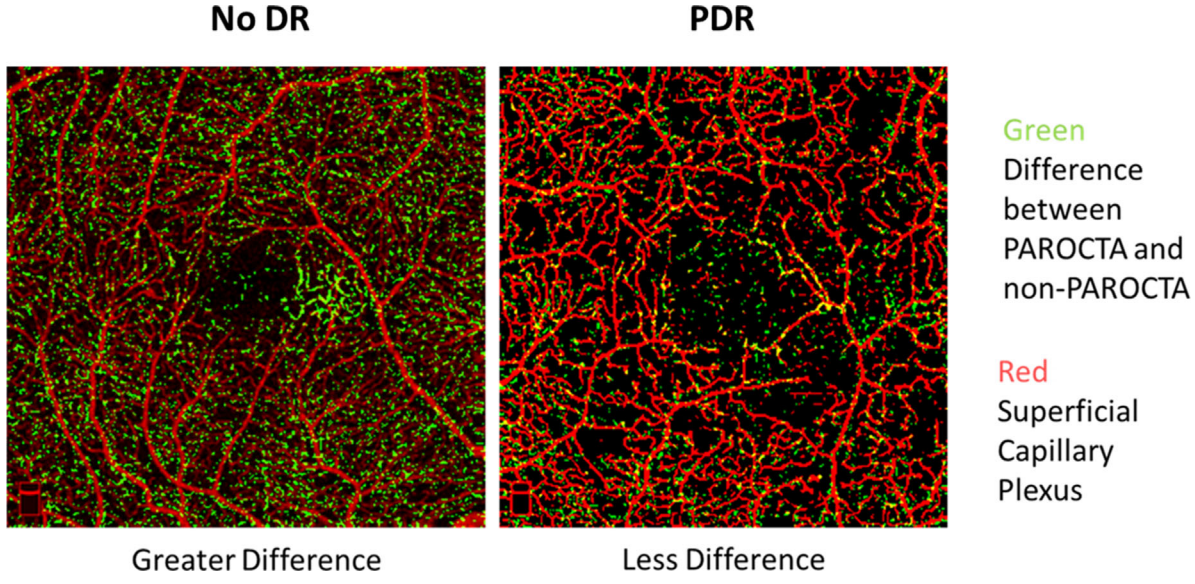

Figure 6. Image demonstrating that pixels unique to projection artifact removal optical coherence tomography angiography (PAROCTA) (green) overlaid on the superficial capillary plexus (SCP) (red) for orientation, demonstrating that there are significantly greater differences in eyes with no diabetic retinopathy (DR) (left hand image) compared to eyes with proliferative diabetic retinopathy (PDR) (right hand image).

increasing DR severity may not occur at similar rates and appear at least partially independent of each other.

Although one might suspect that the removal of projection artifacts would decrease VD measurements in the deeper retinal layers, the opposite was true. VD measurements increased after projection artifact removal, likely because the removal of large vascular artifacts allowed better visualization of the intricate smaller capillaries of the deeper vascular layers and, hence, a higher overall DCP VD (Fig. 6). We also observed that these differences were more significant in eyes with no DR and mild NPDR, perhaps as a result of the relative preservation of the SCP in eyes with less severe DR, leading to more extensive projection artifacts and a more substantial effect after subsequent removal (Fig. 6). Another possibility is that with increasing DR severity, the vascular density of the underlying DCP also decreases and, hence, even after removal of projection artifacts, "recovery" or improved visualization of small capillaries is limited.[31] This concept of small capillary recovery is supported by the finding that these changes are mirrored in both the VD and VLD. VLD is a measure of total vascular length and is a surrogate for the complexity of vascular architecture. The fact that DCP VLD measurements increased on PAROCTA as compared to non-PAROCTA indicates that these differences were driven by the visualization of more blood vessels rather than by simple alterations in the diameter of already visualized vessels.

It might be expected that PAROCTA would mainly alter findings in the deeper vascular layers; however, we also found differences in the SCP after utilizing the new projection artifact removal software. Eyes with more severe DR (moderate NPDR or worse) had significantly lower SCP VD and VLD measurements when using PAROCTA as compared to non-PAROCTA. A possible explanation could lie in the differences in slab segmentation between the two software approaches. Because many of the previous and expected future studies rely on built-in automatic offsets, we did not manually change these offsets for our evaluation of either version of the software.[2,15,30,32] Nonetheless, it is critical to recognize that in the non-PAROCTA software, the outer boundary of the SCP slab is 15 µm below the IPL, whereas that of the PAROCTA is 10 µm above it. This may result in the non-PAROCTA software capturing significantly more of the intermediate capillary plexus given its location in the IPL and inner nuclear layer (INL). The differential changes with DR severity may be partly explained by previous work demonstrating that increasing DR severity is associated with inner retinal thinning of the ganglion cell-IPL layer causing the ICP to feature more prominently in the SCP slab of non-PAROCTA.[33,34] In contrast, we hypothesize that the difference in segmentation for the inner boundary at the ILM will probably be less impactful because it is only shifted approximately 3 microns and the average diameter of capillaries is 5 to 7 µm. To test this hypothesis, we ran a subgroup analysis with 25 eyes that had the greatest SCP VD difference between PAROCTA and non-PAROCTA. When utilizing PAROCTA analysis with the non-PAROCTA offsets, SCP VD measurements were significantly greater than they were when using PAROCTA analysis with the default PAROCTA offsets (35.43 ± 3.74 vs. 29.29 ± 3.65, $P < 0.001$ paired t-test). This suggests that the posterior offset location had a significant effect that was independent of other software differences.

Some studies have relied on full thickness retinal slabs to evaluate VD changes in DR given that full thickness segmentation might enable more accurate quantification of vascular parameters in the presence of macular edema and/or segmentation errors.[35,36] Although it is assumed that the projection artifact removal would not affect these measurements, this has not previously been fully evaluated. In the current study, there was no significant difference between PAROCTA and non-PAROCTA VD and VLD, except in eyes with no DR and to a lesser extent in eyes with moderate NDPR. This again could be related to projection artifact removal from deeper layers allowing the unmasking and visualization of deeper capillaries. However, we are unsure why no difference was seen in eyes with mild NDPR. We also evaluated AFI, which has been previously evaluated as a surrogate for flow, but, in this case, was used to evaluate overall pixel intensity. As expected, pixel intensity of PAROCTA images was significantly lower that non-PAROCTA, which is not surprising because full thickness slabs incorporate both SCP and DCP projection artifacts, which should be significantly reduced in PAROCTA images. Therefore, results of AFI from non-PAROCTA studies should not be automatically extrapolated to PAROCTA findings.

There was a weak positive correlation between SSI and the difference in PAROCTA and non-PAROCTA VD in the SCP (0.200, $P < 0.001$) and a weak negative correlation for the same difference in the DCP (-0.138, $P = 0.013$). However, SSI was not significantly different between the different DR groups and an SSI threshold of ≥ 60 was used for study inclusion.

Strengths of this study include the large number of eyes in each DR severity level which allowed the evaluation of non-PAROCTA and PAROCTA assessment within each individual DR severity as well as

the comparison of differences between different DR severity levels. All eyes were graded for DR severity using UWF imaging by a trained masked grader using standardized grading techniques. Eyes with macular edema were excluded from the study, therefore, limiting possible artifacts and segmentation errors that may affect VD and VLD measurements. The same eye of the same patient was used to compare between the PAROCTA and non-PAROCTA, thus limiting the effect of confounding factors that may affect OCTA measurements, such as age, sex, A1c, and duration of DM.[37,38] Limitations of the current study include the manual processing of the images, although this technique has been previously validated and it consists of a group of sequential standardized image processing steps requiring no subjective input from the user. Nonetheless, the output from this method is not identical to that obtained with the automated vessel quantification software currently available on the OCTA device.[10] The use of manual processing was necessary because of the lack of availability of automatic VD measurements for the DCP in our non-PAROCTA software. We ran correlations between the SCP manual and automatic measurements and found them highly correlated in both PAROCTA and non-PAROCTA. Therefore, manual image analysis can likely be extrapolated to the automatic VD provided by the new software. In a study comparing five different binarization techniques by Mehta et al., no specific advantage for one technique was found. However, the study recommended that for a given cohort the same technique should be used across all images. In the current study we utilized the same binarization technique for both the PAROCTA and the non-PAROCTA images thereby limiting any potential confounding effect of different binarization techniques on the outcomes of the study.[39]

These findings indicate that OCTA projection artifact removal differentially impacts SCP and DCP measurements depending upon the DR severity within a given eye. Furthermore, projection artifact removal may affect full thickness AFI and, to a lesser extent, VD measurements in addition to those for individual capillary layers. Given that multiple previous studies evaluating the relationship of VD and DR severity level have not used PAR, conclusions drawn from those data with regard to the role of specific vascular layers in DR should be carefully reviewed with this interaction in mind and direct comparison between PAROCTA and non-PAROCTA studies may not be appropriate. As OCTA image analysis evolves, evaluation of future software iterations should include eyes across the spectrum of DR severity, rather than generalizing from a specific retinopathy subgroup.

Acknowledgments

Supported by NEI R01 EY024702, Research to Prevent Blindness, Massachusetts Lions Eye Research Fund, and Optovue.

Disclosure: **M. Ashraf**, None; **K. Sampani**, None; **O. Abu-Qamar**, None; **J. Cavallerano**, None; **P.S. Silva**, None; **L.P. Aiello**, None; **J.K. Sun**, Optovue (F)

References

1. Jia Y, Tan O, Tokayer J, et al. Split-spectrum amplitude-decorrelation angiography with optical coherence tomography. *Optics Express*. 2012;20:4710–4725.
2. Dimitrova G, Chihara E, Takahashi H, Amano H, Okazaki K. Quantitative retinal optical coherence tomography angiography in patients with diabetes without diabetic retinopathy. *Invest Ophthalmol Vis Sci*. 2017;58:190–196.
3. Vujosevic S, Muraca A, Alkabes M, et al. Early microvascular and neural changes in patients with type 1 and type 2 diabetes mellitus without clinical signs of diabetic retinopathy. *Retina*. 2019;39:435–445.
4. Spaide RF, Fujimoto JG, Waheed NK. Image artifacts in optical coherence tomography angiography. *Retina*. 2015;35:2163–2180.
5. Spaide RF, Fujimoto JG, Waheed NK, Sadda SR, Staurenghi G. Optical coherence tomography angiography. *Prog Retin Eye Res*. 2018;64:1–55.
6. Hwang TS, Zhang M, Bhavsar K, et al. Visualization of 3 distinct retinal plexuses by projection-resolved optical coherence tomography angiography in diabetic retinopathy. *JAMA Ophthalmol*. 2016;134:1411–1419.
7. Zhang M, Hwang TS, Dongye C, Wilson DJ, Huang D, Jia Y. Automated quantification of nonperfusion in three retinal plexuses using projection-resolved optical coherence tomography angiography in diabetic retinopathy. *Invest Ophthalmol Vis Sci*. 2016;57:5101–5106.
8. Zhang M, Hwang TS, Campbell JP, et al. Projection-resolved optical coherence tomographic angiography. *Biomed Opt Express*. 2016;7:816–828.
9. Zhang A, Zhang Q, Wang RK. Minimizing projection artifacts for accurate presentation of choroidal neovascularization in OCT micro-

angiography. *Biomed Opt Express*. 2015;6:4130–4143.

10. Garrity ST, Iafe NA, Phasukkijwatana N, Chen X, Sarraf D. Quantitative analysis of three distinct retinal capillary plexuses in healthy eyes using optical coherence tomography angiography. *Invest Ophthalmol Vis Sci*. 2017;58:5548–5555.
11. Samara WA, Shahlaee A, Adam MK, et al. Quantification of diabetic macular ischemia using optical coherence tomography angiography and its relationship with visual acuity. *Ophthalmology*. 2017;124:235–244.
12. Kim AY, Chu Z, Shahidzadeh A, Wang RK, Puliafito CA, Kashani AH. Quantifying microvascular density and morphology in diabetic retinopathy using spectral-domain optical coherence tomography angiography. *Invest Ophthalmol Vis Sci*. 2016;57:Oct362–Oct370.
13. Al-Sheikh M, Akil H, Pfau M, Sadda SR. Swept-source OCT angiography imaging of the foveal avascular zone and macular capillary network density in diabetic retinopathy. *Invest Ophthalmol Vis Sci*. 2016;57:3907–3913.
14. Ashraf M, Nesper PL, Jampol LM, Yu F, Fawzi AA. Statistical model of optical coherence tomography angiography parameters that correlate with severity of diabetic retinopathy. *Invest Ophthalmol Vis Sci*. 2018;59:4292–4298.
15. Agemy SA, Scripsema NK, Shah CM, et al. Retinal vascular perfusion density mapping using optical coherence tomography angiography in normals and diabetic retinopathy patients. *Retina*. 2015;35:2353–2363.
16. Park JJ, Soetikno BT, Fawzi AA. Characterization of the middle capillary plexus using optical coherence tomography angiography in healthy and diabetic eyes. *Retina*. 2016;36:2039–2050.
17. Lee J, Moon BG, Cho AR, Yoon YH. Optical coherence tomography angiography of DME and its association with anti-VEGF treatment response. *Ophthalmology*. 2016;123:2368–2375.
18. Lee J, Rosen R. Optical coherence tomography angiography in diabetes. *Curr Diab Rep*. 2016;16:123.
19. Bhanushali D, Anegondi N, Gadde SG, et al. Linking retinal microvasculature features with severity of diabetic retinopathy using optical coherence tomography angiography. *Invest Ophthalmol Vis Sci*. 2016;57:Oct519–Oct525.
20. Dupas B, Minvielle W, Bonnin S, et al. Association between vessel density and visual acuity in patients with diabetic retinopathy and poorly controlled type 1 diabetes. *JAMA Ophthalmology*. 2018;136:721–728.
21. Zhu T, Ma J, Li J, et al. Multifractal and lacunarity analyses of microvascular morphology in eyes with diabetic retinopathy: a projection artifact resolved optical coherence tomography angiography study. *Microcirculation*. 2019;26:e12519.
22. Fawzi AA, Fayed AE, Linsenmeier RA, Gao J, Yu F. Improved macular capillary flow on optical coherence tomography angiography after panretinal photocoagulation for proliferative diabetic retinopathy. *Am J Ophthalmol*. 2019;206:217–227.
23. Lavia C, Couturier A, Erginay A, Dupas B, Tadayoni R, Gaudric A. Reduced vessel density in the superficial and deep plexuses in diabetic retinopathy is associated with structural changes in corresponding retinal layers. *PLoS One*. 2019;14:e0219164.
24. Simonett JM, Scarinci F, Picconi F, et al. Early microvascular retinal changes in optical coherence tomography angiography in patients with type 1 diabetes mellitus. *Acta Ophthalmologica*. 2017;95:e751–e755.
25. Wells JA, Glassman AR, Ayala AR, et al. Aflibercept, bevacizumab, or ranibizumab for diabetic macular edema. *N Engl J Med*. 2015;372:1193–1203.
26. Silva PS, Cavallerano JD, Sun JK, Noble J, Aiello LM, Aiello LP. Nonmydriatic ultrawide field retinal imaging compared with dilated standard 7-field 35-mm photography and retinal specialist examination for evaluation of diabetic retinopathy. *Am J Ophthalmol*. 2012;154:549–559.e542.
27. No authors listed. Grading diabetic retinopathy from stereoscopic color fundus photographs–an extension of the modified Airlie House classification. ETDRS report number 10. Early Treatment Diabetic Retinopathy Study Research Group. *Ophthalmology*. 1991;98(5 Suppl):786–806.
28. Borrelli E, Lonngi M, Balasubramanian S, et al. Macular microvascular networks in healthy pediatric subjects. *Retina*. 2019;39:1216–1224.
29. Uji A, Balasubramanian S, Lei J, Baghdasaryan E, Al-Sheikh M, Sadda SR. Impact of multiple en face image averaging on quantitative assessment from optical coherence tomography angiography images. *Ophthalmology*. 2017;124:944–952.
30. Nesper PL, Roberts PK, Onishi AC, et al. Quantifying microvascular abnormalities with increasing severity of diabetic retinopathy using optical coherence tomography angiography. *Invest Ophthalmol Vis Sci*. 2017;58:BIO307–BIO315.
31. Kashani AH, Chen CL, Gahm JK, et al. Optical coherence tomography angiography: A comprehensive review of current methods and clinical applications. *Prog Retin Eye Res*. 2017;60:66–100.

32. Scarinci F, Nesper PL, Fawzi AA. Deep retinal capillary nonperfusion is associated with photoreceptor disruption in diabetic macular ischemia. *Am J Ophthalmol*. 2016;168:129–138.
33. Ng DS, Chiang PP, Tan G, et al. Retinal ganglion cell neuronal damage in diabetes and diabetic retinopathy. *Clin Exp Ophthalmol*. 2016;44:243–250.
34. Campbell JP, Zhang M, Hwang TS, et al. Detailed vascular anatomy of the human retina by projection-resolved optical coherence tomography angiography. *Sci Rep*. 2017;7:42201.
35. Lin AD, Lee AY, Zhang Q, et al. Association between OCT-based microangiography perfusion indices and diabetic retinopathy severity. *Br J Ophthalmol*. 2017;101:960–964.
36. Schottenhamml J, Moult EM, Ploner S, et al. An automatic, intercapillary area-based algorithm for quantifying diabetes-related capillary dropout using optical coherence tomography angiography. *PLoS One*. 2016;36(Suppl 1):S93–s101.
37. Leng Y, Tam EK, Falavarjani KG, Tsui I. Effect of age and myopia on retinal microvasculature. *Ophthalmic Surg Lasers Imaging Retina*. 2018;49:925–931.
38. Dervenis N, Harris A, Coleman AL, et al. Factors associated with non-active retinal capillary density as measured with confocal scanning laser doppler flowmetry in an elderly population: the Thessaloniki Eye Study (TES). *Br J Ophthalmol*. doi:10.1136/bjophthalmol-2019-315212. Online ahead of print.
39. Mehta N, Liu K, Alibhai AY, et al. Impact of binarization thresholding and brightness/contrast adjustment methodology on optical coherence tomography angiography image quantification. *Am J Ophthalmol*. 2019;205:54–65.